Fast Calibration-Free Single-Anchor Indoor Localization Based on Limited Number of ESPAR Antenna Radiation Patterns

Mateusz Groth[1], Krzysztof Nyka[2], *Senior Member, IEEE* and Lukasz Kulas[3], *Senior Member, IEEE*
Department of Microwave and Antenna Engineering,
Faculty of Electronics, Telecommunications and Informatics, Gdansk University of Technology 80-233 Gdansk, Poland,
[1] mateusz.groth@pg.edu.pl, [2] krzysztof.nyka@pg.edu.pl, [3]lukasz.kulas@pg.edu.pl

***Abstract*— In this article, we investigate how the calibration-free single-anchor indoor localization algorithm developed for base stations equipped with electronically steerable parasitic array radiator (ESPAR) antennas can further be improved. By reducing the total number of ESPAR antenna radiation patterns used in localization process, one can significantly reduce the time needed for an object localization. Performed localization measurements involved different placement and number of reference nodes (RNs) used by the calibration-free single-anchor indoor localization algorithm, as well as different possible radiation patterns sets involving 6, 4 or 3 radiation patterns. Test results show that without significant deterioration of the overall accuracy one can easily speed up the algorithm execution time.**

***Index Terms*—Switched-beam antenna, reconfigurable antenna, steerable antenna, electronically steerable parasitic array radiator (ESPAR) antenna, indoor localization, RSS.**

I. INTRODUCTION

Indoor positioning systems using radio frequency (RF) wireless communication play an important role in many practical applications [1]-[3]. They can be installed in environments, in which Global Navigation Satellite Systems (GNSS) signals cannot easily be accessed [4], and relying on a dedicated wireless infrastructure installed indoors provide location based services (LBS) that improve safety, efficiency or provide additional profits. One of the most popular positioning solutions operate in a license-free industrial, scientific and medical (ISM) 2.4 GHz frequency band and involve devices based on common standards such as IEEE 802.11, IEEE 802.15.4 or Bluetooth Low Energy (BLE). Unfortunately, most of such systems require many base stations (BSs), which position has to be planned before system deployment. This not only creates high installation costs but also limits system scalability making system extension after the deployment difficult.

Single-anchor indoor localization is an interesting idea of improving scalability and reducing deployment costs of IPS installations [5]-[7]. The concept relies, instead of a set of reference nodes (RNs), on a single 2.4-GHz BS equipped with a switched-beam antenna, which can by its own determine the unknown position of an object with a RF beacon attached by recording received signal strength (RSS) for different antenna radiation patterns. Therefore, the system can easily be extended by simply installing new BSs in places where information about objects' position is required.

One of the most promising realizations of single-anchor localization system rely on low-cost and energy-efficient electronically steerable parasitic array radiator (ESPAR) antenna [7]. The antenna, as presented in Fig. 1, have a centrally placed single active monopole, that can be directly connected to a low-cost wireless transceiver, is surrounded by 12 passive elements which can be electronically switched between shorting to the ground or opening by a simple microcontroller controlling low-cost energy-efficient RF switches connected to the passive elements' ends. By an appropriate configuration of 12 RF switches, one can form a directional radiation pattern and rotate it with a discreet step in the horizontal direction. The application of the design of ESPAR antenna for direction of arrival (DoA) estimation using MUSIC algorithm was initially presented in [8]. Similar designs for DoA applications were presented in [9]-[11]. A single BS using such ESPAR antenna can provide 1.61 m localization error mean value by means of a fingerprinting algorithm [7], however it requires a troublesome calibration.

Recently, a new calibration-free algorithm was proposed for single-anchor indoor localization using ESPAR antennas and additional low-cost BLE modules installed in fixed positions at room walls as auxiliary reference nodes (RN) [8]. The new algorithm not only provides 13,7% lower localization mean error when compared to the fingerprinting method but also does not require laborious calibration and recalibration processes during system deployment and regular recalibrations which are necessary to take the changes in the propagation environment into account.

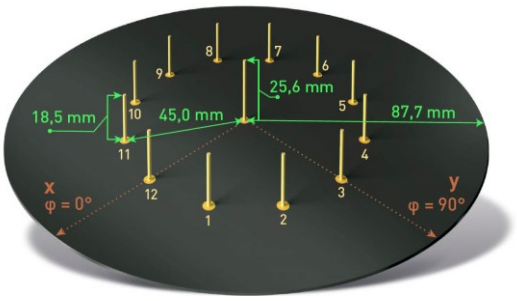

Fig. 1. ESPAR antenna design.

One of the unaddressed issues of currently available algorithms for single-anchor indoor localization is high number of ESPAR antenna radiation patterns that has to be used to find an unknown object position. This directly influences time necessary to collect all RSS measurements and, therefore, it limits possible applications to those in which objects having RF beacons attached do not move fast. In this paper, we investigate how the reduced number of ESPAR antenna radiation patterns together with BLE reference tags placement influences the overall accuracy of calibration-free single-anchor indoor localization using ESPAR antenna. In result, we show how to limit the number of necessary RSS measurement and make the localization algorithm much faster without significant deterioration of the overall accuracy.

II. ESPAR ANTENNA

The ESPAR antenna used in the presented localization system consists of an active element, located in the middle, and 12 passive elements around it. Each passive element can be switched between a short and open through single-pole double-throw (SPDT) FET switches, controlled from the microcontroller. With such the design, it is possible to achieve 12 directional radiation patterns that additionally can be rotated with a $\mathbf{30}°$ step [7],[8].

The antenna, presented in Fig. 1, is designed for the center frequency of 2.484 GHz has the 3dB beamwidth of $\mathbf{73.2}°$ for directional pattern, shown in Fig. 2, which can be achieved by shorting five adjacent passive elements. Each antenna radiation pattern can be described by the steering vector $\mathbf{V^n_{max}} = [\boldsymbol{v_1}\, \boldsymbol{v_2} \cdots \boldsymbol{v_s} \cdots \boldsymbol{v_{11}}\, \boldsymbol{v_{12}}]$ where $\boldsymbol{v_s} = \mathbf{0}$ when the sth element is shorted and $\boldsymbol{v_s} = \mathbf{1}$ when opened. The corresponding vectors together with main beam directions are presented in Table I.

TABLE I. STEERING VECTORS FOR MAIN BEAM DIRECTIONS

n	φ^n_{max}	V^n_{max}
1	90°	111110000000
2	120°	011111000000
3	150°	001111100000
4	180°	000111110000
5	210°	000011111000
6	240°	000001111100
7	270°	000000111110
8	300°	000000011111
9	330°	100000001111
10	0°	110000000111
11	30°	111000000011
12	60°	111100000001

Antenna prototype was realized using 1.55 mm FR4 laminate. Copper rod of 2 mm diameter was used for active and passive elements. For the switching functionality, NJG1681MD7 GaAs FET MMICs SPDT switches have been used.

III. CALIBRATION-FREE POSITIONNG ALGORITHM

A. The algorithm

The positioning algorithm, initially proposed in [12], benefits from fingerprinting and trilateration concepts and utilizes the directivity of the antenna to estimate the most possible direction of the localized device. For that, the proposed method uses static RNs of known location to neutralize the negative influence of RF propagation phenomena, such as reflections or local attenuations. Each RN is a simple active BLE transmitters that periodically sends signals which received signal strength (RSS) is measured in the BS equipped with ESPAR antenna. RSS for each antenna radiation pattern is stored in the database and can be denoted as a vector:

$$\mathbf{V}_{ref_j} = [RSS_{ref_{j_1}}, \dots, RSS_{ref_{j_i}}, \dots, RSS_{ref_{j_{12}}}] \quad (1)$$

where $RSS_{ref_{j_i}}$ is jth RN RSS value for the ith antenna configuration. Similarly, a vector for the localized node can be denoted as:

$$\mathbf{V}_{loc} = [RSS_{loc_1}, \dots, RSS_{loc_i}, \dots, RSS_{loc_{12}}] \quad (2)$$

where RSS_{loc_i} is the RSS value for ith antenna configuration.

The localization procedure is divided into two steps. In the first one, the distance between reference nodes and localized node is estimated. For that, Euclidean distance D_j between $\mathbf{V}_{ref_j}$ and $\mathbf{V}_{loc}$ for each jth RN is calculated:

$$D_j = \left\| \mathbf{V}_{loc} - \mathbf{V}_{ref_j} \right\| = \sqrt{\sum_{i=1}^{12} \left(RSS_{loc_i} - RSS_{ref_{j_i}} \right)^2} \quad (3)$$

The distances can be ordered by their value:

$$D_{j=k_1} \le D_{j=k_2} \le D_{j=k_3} \le \cdots \le D_{j=k_J} \quad (4)$$

where J is a total number of reference nodes and $k_1, \dots, k_J$ are indices of the distances sorted ascending. During the second step, K reference nodes of the lowest calculated distance $\{D_{j=k_1}, D_{j=k_2}, \dots, D_{j=k_K}\}$ are chosen. The position of localized nodes is estimated using Weighted K-nearest neighbors method, for which weight of each node is calculated as:

$$w_j = \frac{D_j}{\sum_{i=1}^{K} D_{k_i}} \quad (5)$$

for $j = \{k_1, \dots, k_K\}$, where K is the number of reference nodes chosen for the second phase. Finally, the position of a localized node is estimated as:

$$(x, y) = \left(\sum_{j=k_1}^{k_K} w_j x_j \, , \sum_{j=k_1}^{k_K} w_j y_j \right) \quad (6)$$

where (x_n, y_n) are the coordinates of jth reference node.

B. The algorithm for reduced number radiation patterns

By default, for each reference and localized node, RSS values are measured for 12 radiation patterns. As the localization algorithm is relatively fast and simple, RSS measurements that are required for each of the radiation patterns are the biggest contributors to the overall localization time. By limiting number of radiation patterns one can easily speed up the whole algorithm. To this end, we propose to investigate the overall performance when 6, 4, and 3 radiation patterns with equal angular distance between main beams are used, as presented in Fig. 2 and Table II. By reducing the number of radiation patterns, the estimation time reduces as the system measures and collects fewer RSS values for each reference and localized node, which can be denoted as:

$$\mathbf{V}_{ref_j} = [RSS_{ref_{j_1}}, RSS_{ref_{j_2}}, \dots, RSS_{ref_{j_m}}] \quad (7)$$

$$\mathbf{V}_{loc} = [RSS_{loc_1}, RSS_{loc_2}, \dots, RSS_{loc_m}] \quad (8)$$

where $m \in \{3, 4. 6\}$ is the number of radiation patterns used in the localization algorithm. Moreover, one should note that for a certain m, the total number of available radiation pattern sets is $12/m$ while the angular distance between them is $360°/m$ as presented in Table II.

TABLE II. NUMBER OF CONSIDERED RADIATION PATTERNS USED FOR THE EXPERIMENT (SEE TEXT FOR EXPLANATIONS)

m	Angular distance between radiation patterns used	Number of radiation patterns considered for estimation	The total number of radiation pattern sets available
6	60°	6	2
4	90°	4	3
3	120°	3	4

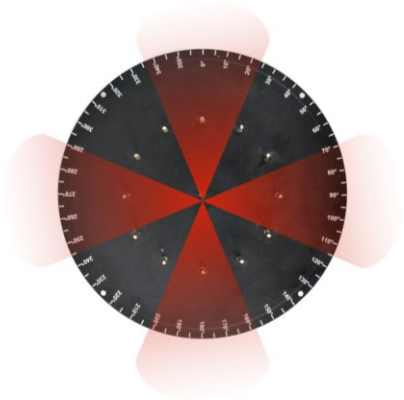

Fig. 2. Examplary set of 4 radiation patterns of ESPAR antenna .

IV. TEST RESULTS

A. Test environment

For the test, the same setup as described in [12]was used to provide a fair comparison. The equipment consisted of ESPAR antenna connected to a WSN module equipped with BLE Nordic nRF52840 SoC and 25 Nordic nRF52840 dongles, each equipped with integrated PCB 2.4 GHz antenna, serving as reference and localized nodes.

Experiments were conducted in $5.6\ \text{m} \times 6.6\ \text{m}$ class room, where the base station was installed on the ceiling in the center of the room, while 24 reference nodes were located evenly on the walls at the height of 1.5 meters. Modules were set to advertising mode with the transmission power of 0 dBm. Additionally, all the modules were set to the Bluetooth channel number 38.

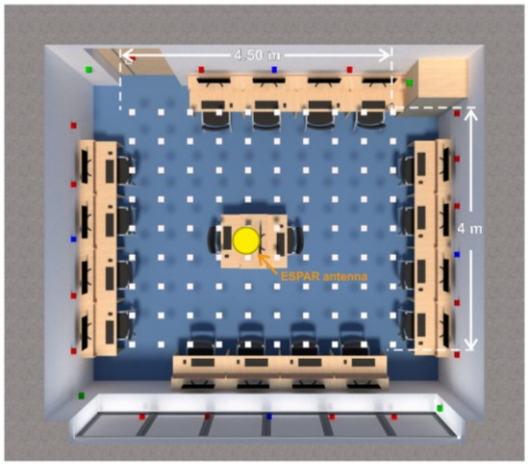

Fig. 3. Plan of the test environment with reference nodes (red, green and blue squares) and test positions (white squares)

B. Test procedure

For the evaluation, the localized module was placed on a gird of $4.5\ \text{m} \times 4\ \text{m}$ with 0.5 m step. For each test position, localized and reference nodes were transmitting BLE packets that were received by the ESPAR antenna. In every location, RSS values for 100 transmitted packets from reference and localized node were measured for each of 12 ESPAR antenna radiation patterns and stored in the database. In the same position, the measurements were taken for sets of 3, 4 and 6 equally distributed ESPAR antenna configurations, as presented in Fig 2. For each set, the measurements were taken for all the possible layouts for the considered number of radiation patterns by rotating them to obtain all the possible sets of patterns, as presented in Fig. 4. As a result, data for total of 9 sets of ESPAR antenna characteristics were collected.

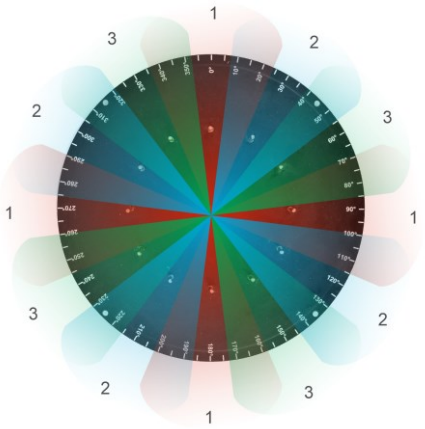

Fig. 4. Considered sets of 4 radiation patterns of the ESPAR antenna. Each set described with different color (red, blue and green) and set's number.

V. RESULTS

For each test point, an error distance was calculated as a difference between estimated an actual position of localized node. Then, the mean value of all the error distances for each ESPAR antenna radiation pattern set was calculated. In Table III, the results for both possible sets of evenly spread 6 antenna characteristics are presented together with the reference results for 12 characteristics from [12].

TABLE III. MEAN VALUE OF ERROR CALCULATED FOR 2 SETS WHEN 6 ESPAR ANTENNA RADIATION PATTERNS ARE USED

reference nodes configuration	12 antenna char. mean error [cm] (results from [8])	6 antenna char. mean error [cm]	
		Set 1	Set 2
corners (4 modules)	163	158	168
middle (4 modules)	139	139	141
corners and middle (8 modules)	184	190	198
all (24 modules)	199	204	209

As one can easily notice, reduction of number of radiation patterns by half does not influence much on the results as the mean error values for each reference modules configuration and number of RNs considered for the positioning algorithm K are similar to those achieved for 12 antenna characteristics. In Fig. 5, cumulative distribution function for both sets of ESPAR radiation patterns is presented that confirms the obtained results. From the graph, one can easily read that for both sets, the estimation error is less than 2 meters for about 80% of test points.

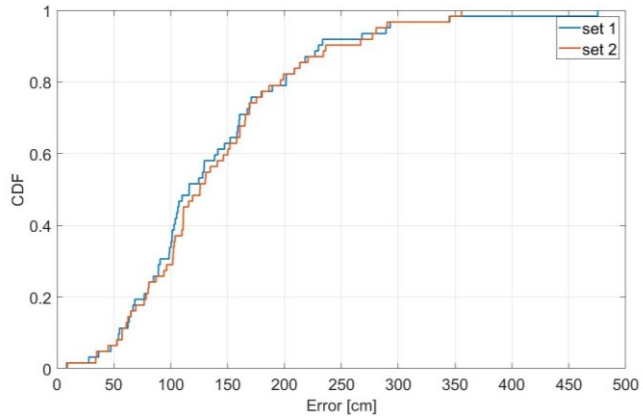

Fig. 5. Localization errors in a form of cumulative distribution function for 6 ESPAR antenna radiaiton patterns considered.

Further tests were conducted for the sets having 4 and 3 ESPAR antenna radiation patterns. They are shown in Table IV and Fig. 6 for sets having 4 radiation patterns, and Table V and Fig. 7 for sets having 3 radiation patterns.

TABLE IV. MEAN VALUE OF ERROR CALCULATED FOR 3 SETS WHEN 4 ESPAR ANTENNA RADIATION PATTERNS ARE USED

reference nodes configuration	4 antenna char. mean error [cm]		
	Set 1	Set 2	Set 3
corners (4 modules)	168	186	157
middle (4 modules)	143	143	144
corners and middle (8 modules)	188	202	186
all (24 modules)	201	204	187

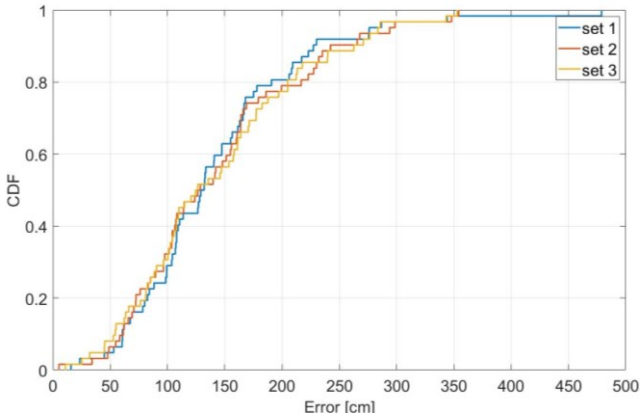

Fig. 6. Localization errors in a form of cumulative distribution function for 4 ESPAR antenna radiaiton patterns considered.

TABLE V. MEAN VALUE OF ERROR CALCULATED FOR 4 SETS WHEN 3 ESPAR ANTENNA RADIATION PATTERNS ARE USED

reference modules configuration	3 antenna char. mean error [cm]			
	Set 1	Set 2	Set 3	Set 4
corners (4 modules)	182	168	152	168
middle (4 modules)	158	160	129	137
corners and middle (8 modules)	205	175	186	199
all (24 modules)	211	190	207	205

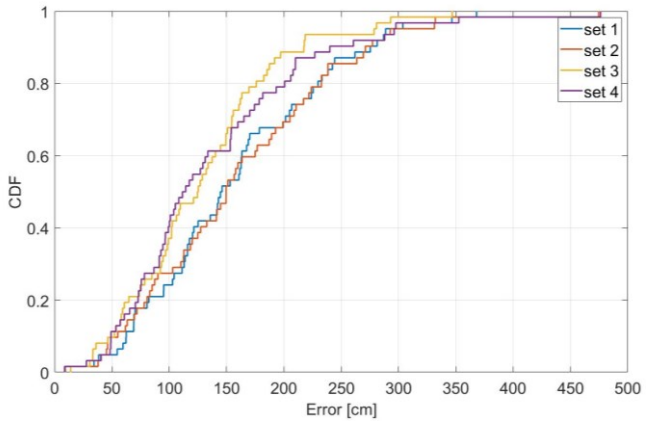

Fig. 7. Localization errors in a form of cumulative distribution function for 3 ESPAR antenna radiaiton patterns considered.

It can easily be noticed, that for each analyzed case the best results were achieved for the setup of reference modules installed in the middle of each wall. This confirms the results described in [12]. Additionally, one can observe that the results obtained for 4 and 3 considered antenna characteristics provide similar results to those obtained with the initial setup of 12 radiation patterns. Moreover, for the setting of three radiation pattern one can select a set that provides better results than when 12 radiations are used. For the considered setup, the reduction from 12 radiation pattern used for the estimation down to 3 results in the reduction of estimation time by about 70%.

VI. CONCLUSION

In this paper, we investigate how a significant reduction of the number of radiation patterns used in BSs equipped with ESPAR antennas for finding an unknown object position of objects impacts calibration-free single-anchor indoor localization algorithm accuracy, initially presented in [12]. Based on measurements involving radiation patterns sets having 6, 4 or 3 radiation patterns, the overall algorithm's performance in terms of cumulative distribution function and mean error values has been calculated for scenario using different RN placement. The results obtained for 3 ESPAR antenna directional radiation patterns provide error levels similar to those obtained by using 12 radiation patterns. It means that the execution speed of the original calibration-free single-anchor indoor localization algorithm can easily be increased. In turn, the proposed improved algorithm can be used in new applications areas, in which the objects with attached BLE localization tags are allowed to move faster.

ACKNOWLEDGMENT

This paper is a result of the InSecTT project which has received funding from the ECSEL Joint Undertaking (JU) under grant agreement No 876038. The JU receives support from the European Union's Horizon 2020 research and innovation programme and Austria, Sweden, Spain, Italy, France, Portugal, Ireland, Finland, Slovenia, Poland, Netherlands, Turkey.

REFERENCES

[1] Stavrou, V.; Bardaki, C.; Papakyriakopoulos, D.; Pramatari, K. An Ensemble Filter for Indoor Positioning in a Retail Store Using Bluetooth Low Energy Beacons. Sensors 2019, 19, 4550, doi:10.3390/s19204550.

[2] Zhang, C.; Qin, N.; Xue, Y.; Yang, L. Received Signal Strength-Based Indoor Localization Using Hierarchical Classification. Sensors 2020, 20, 1067, doi:10.3390/s20041067.

[3] Li, F.; Liu, M.; Zhang, Y.; Shen, W. A Two-Level WiFi Fingerprint-Based Indoor Localization Method for Dangerous Area Monitoring. Sensors 2019, 19, 4243, doi:10.3390/s19194243.

[4] Ochiai, M.; Fujii, M.; Ito, A.; Watanabe, Y.; Hatano, H. A Study on Indoor Position Estimation Based on Fingerprinting Using GPS Signals. In Proceedings of the 2014 International Conference on Indoor Positioning and Indoor Navigation (IPIN); IEEE: Busan, South Korea, October 2014; pp. 727–728.

[5] G. Giorgetti, A. Cidronali, S. Gupta and G. Manes, "Single-anchor indoor localization using a switched-beam antenna", IEEE Commun. Lett., vol. 13, no. 1, pp. 58-60, Jan. 2009.

[6] F. Viani, "Exploitation of parasitic smart antennas in wireless sensor networks", J. Electromagn. Waves Appl., vol. 24, no. 7, pp. 993-1003, Jan. 2010.

[7] M. Rzymowski, P. Woznica and L. Kulas, "Single-Anchor Indoor Localization Using ESPAR Antenna," in IEEE Antennas and Wireless Propagation Letters, vol. 15, pp. 1183-1186, 2016.

[8] E. Taillefer, C. Plapous, J. Cheng, K. Iigusa, and T. Ohira, "Reactancedomain MUSIC for ESPAR antennas (experiment)," in Proc. IEEE Wireless Communications and Networking Confe., vol. 1, New Orleans, LA, Mar. 2003, pp. 98–102.

[9] E. Taillefer, A. Hirata and T. Ohira, "Direction-of-arrival estimation using radiation power pattern with an ESPAR antenna," IEEE Transactions on Antennas and Propagation, vol. 53, no. 2, pp. 678–684, Feb. 2005.

[10] M. Nazaroff, G. Byun, H. Coo, J. Shin and Y. Kim, "2-D Direction of arrival estimation system using circular array with mutually coupled reference signal", IEEE Sensors Journal, vol. 18, pp. 9763-9769, Dec. 2018.

[11] M. Groth, M. Rzymowski, K. Nyka and L. Kulas, "ESPAR Antenna-Based WSN Node With DoA Estimation Capability," in IEEE Access, vol. 8, pp. 91435-91447, 2020, doi: 10.1109/ACCESS.2020.2994364.

[12] M. Groth, K. Nyka, and L. Kulas, "Calibration-Free Single-Anchor Indoor Localization Using an ESPAR Antenna," Sensors, vol. 21, no. 10, p. 3431, May 2021, doi: 10.3390/s21103431. [Online]. Available: http://dx.doi.org/10.3390/s21103431